Design and Fabrication of Extended-Bandwidth Rugate Filters Made of Porous Silicon

Ishikura, Nobuyuki ; Fujii, Minoru ; Nishida, Kohei ; Hayashi, Shinji ; Diener, Joachim ; Mizuhata, Minoru ; Deki, Shigehito

(Citation)
ECS Transactions,16(3):55-59

(Issue Date)
2008

(Resource Type)
journal article

(Version)
Version of Record

(URL)
https://hdl.handle.net/20.500.14094/90005889

ECS Transactions, 16 (3) 55-59 (2008)
10.1149/1.2982541 ©The Electrochemical Society

Design and Fabrication of Extended-Bandwidth Rugate Filters Made of Porous Silicon

N. Ishikura[a], M. Fujii[a], K. Nishida[a], S. Hayashi[a], J. Diener[b], M. Mizuhata[c], S. Deki[c]

[a] Department of Electrical and Electronic Engineering, Graduate School of Engineering, Kobe University, Rokkodai, Nada, Kobe 657-8501, Japan
[b] Physik-Department E16, Technische Universität München, D-85747 Garching, Germany
[c] Department of Chemical Science and Engineering, Graduate School of Engineering, Kobe University, Rokkodai, Nada, Kobe 657-8501, Japan

We designed and fabricated porous silicon-based broadband rugate filters by combining up to seven rugate structures. A near-infrared stop-band filter having a reflection band width of 1926 nm with no higher-order harmonics and very small sidelobes were realized. The suppression of higher-order harmonics and the reduction of sidelobes also allowed us to produce a high quality pass-band filter having three high transmittance regions consisting of broad stop-bands.

Introduction

A rugate filter is a kind of interference filter characterized by a continuous sinusoidal index variation in the direction perpendicular to the film plane (1). It shows a high reflectivity "stop-band" in a specific range of wavelength. Advantages of the rugate filter to discrete multilayer filters consisting of alternating high and low refractive indices layers are a smaller sensitivity to angle variation of incidence light (2) and a suppression of higher-order harmonics. The drawback is its difficulty in realizing the complex refractive index profile with a great accuracy. Usually, the complex refractive index profile is achieved by continuous variation in composition or the density of the filter material (3-6).

Porous silicon produced by electrochemical etching of a silicon wafer is a material of great interest for the fabrication of rugate filters. The refractive index of porous silicon can be controlled by the porosity, which is determined by the current density during the electrochemical etching process (7). The electrochemical etching proceeds only at the etching front and thus already etched layers are unaffected by subsequent etching. These properties make porous silicon an almost ideal system to realize one-dimensional smooth refractive index profiles. In fact, several types of porous silicon-based rugate filters have been reported so far (8-10).

Some applications of a rugate filter, e.g. pass-band, stop-band and edge filters, require wide stop-bands. The width of the stop-band depends on the contrast of the refractive index in a rugate filter. Since the refractive index contrast of a rugate filter made of porous silicon is limited in the range of about 1.3-2.3, it generally has a relatively narrow stop-band. The extension of the rugate stop-band is usually achieved either by a superposition of rugate profiles of different periodicity (4, 11) or by a serial growth of different rugate profiles (12). The combination of the superposition and the serial

methods is also proposed by Southwell (13). The advantage of the combination method is the reduction of the total film thickness. By using the combination method, in a previous work (14), we have succeeded in realizing porous silicon-based broadband rugate filters. The bandwidth reached 1356 nm. This paper is an extension of the previous work. We demonstrate that further extension of the bandwidth is possible by properly controlling the preparation procedure. Furthermore, as an application of the broadband filter a pass-band filter having three transmittance bands is demonstrated.

Experiment

Porous silicon structures were produced by electrochemical etching of (100) oriented p^+ Si wafers (0.02 Ω cm). The etching solution was a 2:3 by volume mixture of HF (46 wt.% in water) and ethanol. The current density was changed from 5 mA/cm^2 to 109 mA/cm^2 with the minimum step of 0.5 mA/cm^2 by computer-controlled current source (Agilent 6612C). In this current density range, the refractive index of porous silicon was changed from 2.38 to 1.30 (at the wavelength of 2 μm). The refractive indices of porous silicon were obtained either from interference patters of uniform layers with known thicknesses or Bruggeman effective medium approximation (15). The total etching time was in the range of 10 to 60 min depending on the structure. During etching, the etching rate decreases slowly (7), i.e., about 1.5 % during the etching of 10 μm. This effect was compensated by controlling the etching time. When free-standing layers were required, porous silicon structures were detached from Si substrates by a high current pulse (400 mA/cm^2, 1.6 s) after finishing the etching procedure. Reflectance and transmittance spectra of porous silicon structures were measured by a UV-visible-NIR spectrophotometer (Shimadzu UV-3101PC) over the spectral range of 350 to 3200 nm with the spectral resolution of 1 nm. The incident angle for the reflectance measurements was 5°.

Results and Discussion

The rugate refractive index profile used in this letter is expressed as

$$n(x) = \exp\left[\frac{\ln n_H + \ln n_L}{2} + \frac{\ln n_H - \ln n_L}{2}\sin\left(\frac{4\pi x}{\lambda_0} + \varphi\right)\right] \qquad [1]$$

where x is the optical path length, n_H and n_L are maximum and minimum refractive indices used in the layer, λ_0 is the wavelength of the stop-band position, and φ is the phase angle (1, 8). To reduce sidelobes that appear on both sides of the stop-band, apodization is applied. We chose a quintic apodization function (16, 17), which shows significant sidelobes suppression properties. A half-apodization technique (18) is also used to reduce total etching time (8). Furthermore, to remove sidelobes caused by large refractive index mismatch between the rugate structure and the surrounding media, the quintic index-matching layers are added to the front and back of the filter. The refractive index profile of the quintic index-matching layer (17) that matches indices form n_1 to n_2 is expressed as

$$n(t) = n_1 + (n_2 - n_1)\left(10t^3 - 15t^4 + 6t^5\right) \qquad [2]$$

where t is the normalized layer thickness, which varies from 0 to 1. In this work, at the interface with air t is varied from 0 to 1, while at that with Si substrate, it is limited from 0 to 0.5 because a full quintic index-matching requires too long etching time when the refractive index of the surround media is very high (8).

Figure 1(a) shows the refractive index profile consisting of seven rugate profiles. To reduce the total film thickness, neighboring rugate profiles are partly overlapped. Each rugate profile consists of 30 periods with quintic apodization and the stop-bands are centered at 1217, 1400, 1610, 1852, 2129, 2449 and 2816 nm. The distances between neighboring stop-bands were determined to be as large as possible to extend the stop-band while keeping the high reflection intensity. Combination of rugate profiles cause optical density minima (dips) in the stop-band. Depths of these dips are usually uneven, but they can be made equal by adjusting the phase (φ) of the rugate profiles [15]. To equalize these dips, the phase is shifted by $\pi/6$ with respect to the neighboring rugate profile. In Fig. 1(b), calculated and measured reflectance spectra are compared. We can see a good agreement between calculated and measured spectra. The width of the stop-band (R>90%) is about 1926 nm. Because of the quintic apodization and indexmatching layers, the sidelobes are rather small.

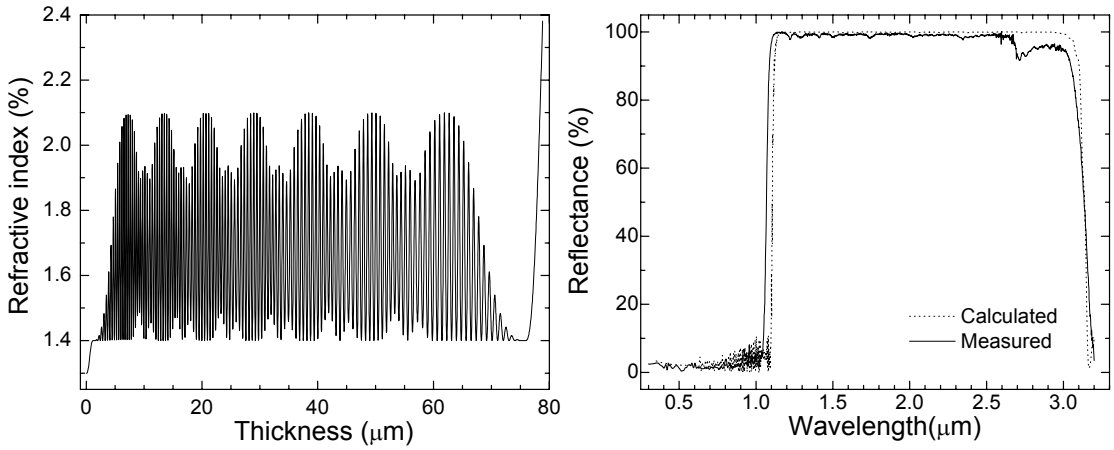

Figure 1. (a) Refractive index profile vs. physical depth and (b) calculated (dotted line) and measured (solid line) reflectance spectra of a rugate structure consisting of seven rugate profiles.

The small sidelobes and higher-order harmonics allow us to make pass-band filters with desired pass-band numbers, positions and widths. As a demonstration we made a pass-band filter with three wide stop-bands. The filter consists of six rugate structures (30 periods) with the stop-bands at 1170, 1346, 1547, 2046, 2353 and 3112 nm (Fig. 2(a)). The filter is detached from the substrate after etching. Fig. 2(b) shows the calculated and measured transmittance spectra. We can see three pass-bands centered at 900, 1780 and 2710 nm sandwiched by broad stop-bands. Note that the stop-band below 800 nm is due to silicon absorption. The pass-band position, width and number can be tailored simply by properly controlling the stop-band positions of rugate structures constructing the filter.

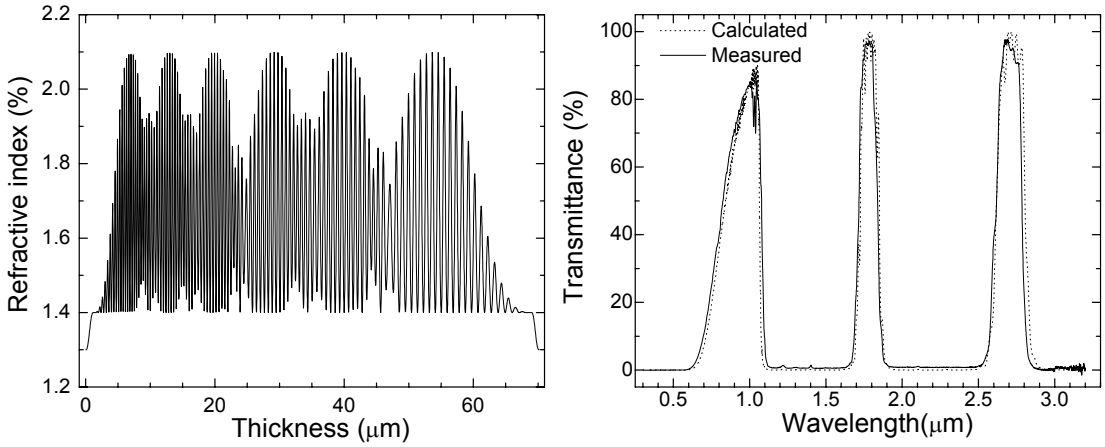

Figure 2. A pass-band filter consisting of six rugate profiles: (a) refractive index profile vs. physical depth and (b) calculated (dotted line) and measured (solid line) transmittance spectra.

Conclusion

By combining seven rugate refractive index profiles, we fabricated a stop-band filter that has a reflection band width of 1926 nm and high transmission region outside the stop-band. A pass-band filter that exhibits three high transmittance regions produced by three broad stop-bands was also demonstrated. The present results demonstrate that the porous silicon-based rugate structures allow us to realize higher-order harmonics free and sidelobes free high quality broadband optical devices by a simple and low-cost process.

Acknowledgments

This work is supported by a Grant-in-Aid for Scientific Research from the Ministry of Education, Culture, Sports, Science and Technology, Japan.

References

1. B. G. Bovard, *Appl. Opt.*, **32**, 5427 (1993).
2. W. H. Southwell, *J. Opt. Soc. Am. A*, **5**, 1558 (1988).
3. K. Kaminska, T. Brown, G. Beydaghyan, and K. Robbie, *Appl. Opt.*, **42**, 4212 (2003).
4. W. J. Gunning, R. L. Hall, F. J. Woodberry, W. H. Southwell, and N. S. Gluck, *Appl. Opt.*, **28**, 2945 (1989).
5. P. L. Swart, P. V. Bulkin, and B. M. Lacquet, *Opt. Eng.*, **36**, 1214 (1997).
6. K. Robbie, A. J. P. Hnatiw, M. J. Brett, R. I. MacDonald, and J. N. McMullin, *Electron. Lett.*, **33**, 1213 (1997).
7. A. G. Cullis, L. T. Canham, and P. D. J. Calcott, *J. Appl. Phys.*, **82**, 909 (1997).
8. E. Lorenzo, C. J. Oton, N. E. Capuj, M. Ghulinyan, D. Navarro-Urrios, Z. Gaburro, and L. Pavesi, *Appl. Opt.*, **44**, 5415 (2005).
9. S. Ilyas, T. Böcking, K. Kilian, P. J. Reece, J. Gooding, K. Gaus, and M. Gal, *Opt. Mater.*, **29**, 619 (2007).
10. M. S. Salem, M. J. Sailor, T. Sakka, and Y. H. Ogata, *J. Appl. Phys.*, **101**, 063503 (2007).

11. J. A. Dobrowolski, and D. Lowe, *Appl. Opt.*, **17**, 3039 (1978).
12. A. G. Imenes, and D. R. McKenzie, *Appl. Opt.*, **45**, 7841 (2006).
13. W. H. Southwell, *Appl. Opt.*, **36**, 314 (1997).
14. N. Ishikura, M. Fujii, K. Nishida, S. Hayashi, J. Diener, M. Mizuhata, and S. Deki, *Opt. Mater.*, to be published.
15. P. A. Snow, E. K. Squire, P. St. J. Russell, and L. T. Canham, *J. Appl. Phys.*, **86**, 1781 (1999).
16. W. H. Southwell, *Appl. Opt.*, **28**, 5091 (1989).
17. W. H. Southwell, *Opt. Lett.*, **8**, 584 (1983).
18. H. A. Abu-Safia, A. I. Al-Sharif, and I. O. Abu Alijarayesh, *Appl. Opt.*, **32**, 4831 (1993).